J|A|C|S
COMMUNICATIONS

Published on Web 10/18/2006

Freestanding Mesoporous Quasi-Single-Crystalline Co_3O_4 Nanowire Arrays

Yanguang Li, Bing Tan, and Yiying Wu*

Department of Chemistry, The Ohio State University, Columbus, Ohio 43210

Received July 24, 2006; E-mail: wu@chemistry.ohio-state.edu

Co_3O_4 is a technologically important material with applications in lithium-ion batteries,[1] gas sensing,[2] and electrochromic devices.[3] Nanostructured Co_3O_4, with a high surface area and enhanced electrochemical reactivity, is particularly attractive for these applications.[1,4] Therefore, its synthesis has been widely explored. For example, one-dimensional (1-D) Co_3O_4 nanotubes and nanowires have been synthesized by using porous alumina[2,5] or virus[6] as templates, or the thermal conversion of cobalt hydroxide nanorods,[7] while other morphologies have also been reported.[8]

For most demonstrated applications of Co_3O_4, electric signals need to either be applied to or be extracted from the active materials. In the case of Li-ion batteries, this is normally achieved by mixing nanostructured Co_3O_4 with carbon and polymer binders and compressing them into pellets.[1] This risks negating the benefits associated with the reduced particle size and introduces supplementary, undesirable interfaces.[9] For these reasons, the direct growth of Co_3O_4 nanowires on various substrates, especially on conducting substrates, is an important issue for their applications.[9,10]

In this communication, we report a facile template-free method for the large-area growth of freestanding hollow Co_3O_4 nanowire arrays on a variety of substrates including transparent conducting glass, Si wafer, and copper foil. More interestingly, these nanowires have the combined properties of mesoporosity and quasi-single-crystallinity. With their high surface area and crystallinity, and their direct growth on conductive substrate, these Co_3O_4 nanowire arrays can be expected to have promising applications in lithium-ion batteries, chemical sensing, and field-emission and electrochromic devices. Using the prepared nanowire arrays as electrode, an electrochemical sensor for hydrogen peroxide sensing has been demonstrated.

The nanowires were synthesized by immersing the selected substrate in a reaction solution contained in a covered petri dish at 90 °C. The reaction solution consisted of $Co(NO_3)_2$ and concentrated aqueous ammonia solution (see Supporting Information for synthesis details). After growth for 14 h, the substrate was covered by a black film, as shown in Figure 1A.

Scanning electron microscopy (SEM) characterization shows that the black film is made up of nanowire arrays with diameters of ~500 nm and lengths up to 15 μm (Figure 1C−F). X-ray diffraction (XRD) pattern shows that the as-made nanowires have the mixed Co_3O_4 spinel phase and β-$Co(OH)_2$ brucite phase (Figure 1B top). FTIR investigation shows that the nanowires also contain NO_3^- ions, possibly intercalated in the layered hydroxide phase (Supporting Information Figure S2). By a subsequent thermal treatment at 250 °C in air, the nanowires are converted into pure spinel phase (Figure 1B middle and bottom spectra). The much stronger (111) peak intensity for the nanowire array in comparison with the powder XRD pattern (Figure 1B, middle vs bottom) strongly indicates that the nanowires grow along the [111] direction, which is confirmed by TEM characterization as shown below.

The nanowire arrays have been successfully grown on Si wafer, microslide, F-doped tin oxide conducting glass, and copper foil, et al. The nanowires, however, cannot grow on Au-coated surface. This phenomenon has been employed to achieve selective nanowire growth on a patterned substrate. Images E and F of Figure 1 show the nanowire growth on a silicon wafer patterned with regularly arranged Au squares. The Co_3O_4 nanowires only grow on regions without Au coating, forming the mesh pattern. This is in contrast to the patterned growth by the vapor−liquid−solid (VLS) mechanism, where nanowires grow only on regions with Au coating.[11]

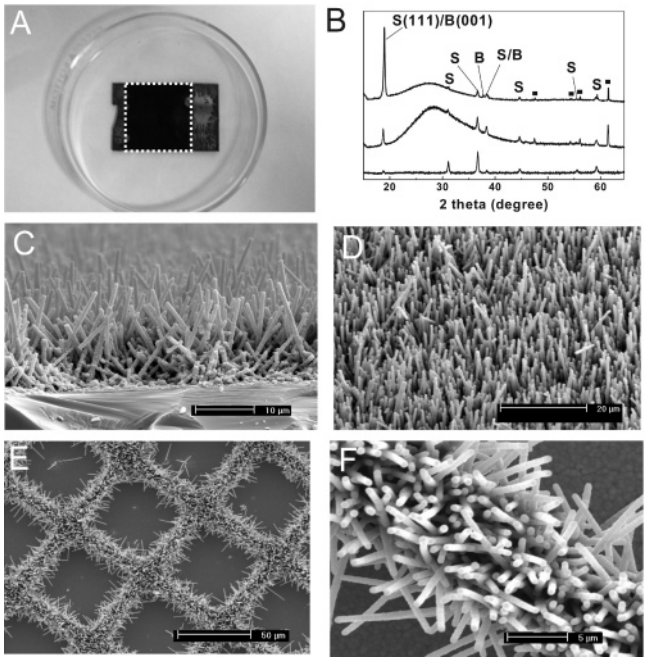

Figure 1. (A) Photograph of the as-made nanowires on Si wafer. The region enclosed by the dotted square was in contact with the solution during growth, while the two sides were clamped by a Teflon holder. (B) XRD patterns of as-made nanowires on Si wafer (top), calcined nanowires on Si wafer (middle), and powders of calcined nanowires scratched down from the substrate (bottom). S and B represent spinel Co_3O_4 and brucite $Co(OH)_2$ phases, respectively. (■) Peaks from substrate. (C−F) SEM images of the nanowire array grown on silicon wafer (C), polystyrene substrate (D), and on Si wafer patterned with Au film (E,F). Nanowires only grow on regions without Au coating; (F) is a close view of the nanowires in (E).

Transmission electron microscopy (TEM) characterization shows that the nanowires have interesting combined properties of porosity and quasi-single-crystallinity (Figure 2). The as-made nanowires have a modulated outer surface profile and hollow interior, as revealed in the side-view TEM image (Figure 2A) and the microtomed cross-section image (Figure 2C). Selected-area electron diffraction (SAED) of a single nanowire (Figure 2D) shows a quasi-single-crystalline pattern with the nanowire growing along [111] direction of the spinel Co_3O_4 structure. Considering the very similar *d*-spacing between the Co_3O_4 spinel (111) planes (4.716 Å, JCPDS 80-1545) and the brucite β-$Co(OH)_2$ (001) planes (4.708 Å, JCPDS 45-0031), the minor β-$Co(OH)_2$ phase may coexist in the nanowires as indicated by the XRD data. This point is explained further in

10.1021/ja065308q CCC: $33.50

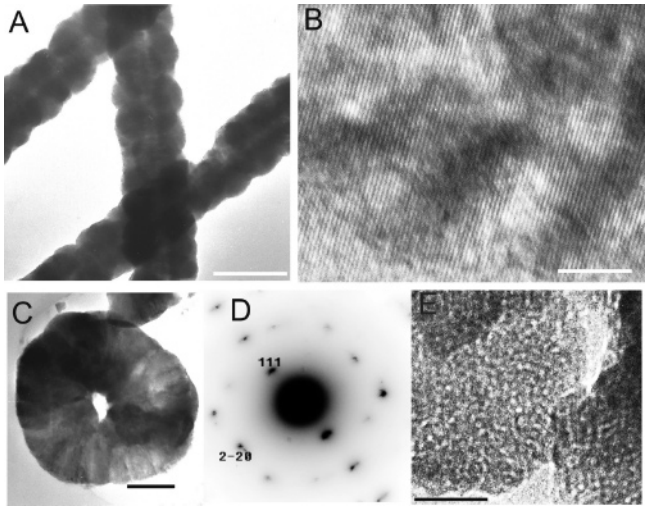

Figure 2. TEM characterization of the Co_3O_4 nanowires. (A) low-magnification image of individual Co_3O_4 nanowires with rippled surface profile and hollow interier. (B) HRTEM image showing both mesopores and the crystalline framework. (C) Microtomed nanowire cross-section showing a hole in the center. (D) SAED pattern of a single nanowire indexed along [11-2] zone axis, and (E) porous nature of the nanowires. Scale bars are (A) 500 nm, (B) 5 nm, (C) 180 nm, and (E) 20 nm.

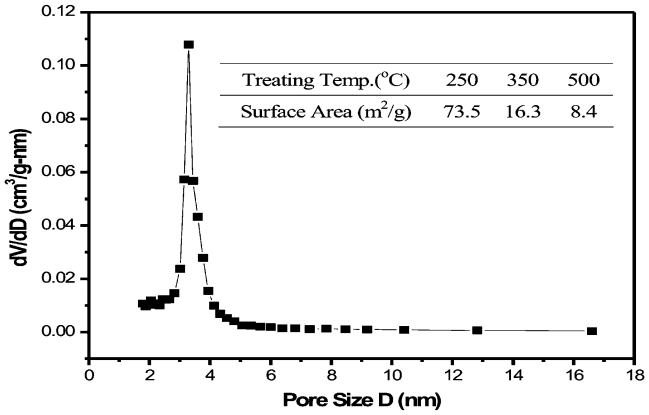

Figure 3. Pore size distribution of Co_3O_4 nanowires after thermal treatment at 250 °C. (Inset table) BET surface area of the nanowires after thermal treatment at the specified temperatures.

the text below. A zoom-in view of the cross-section TEM image shows that the nanowires are mesoporous (Figure 2E) with pore sizes of 3−4 nm. The porosity of the nanowires is maintained after thermal treatment at 250 °C. BET measurement shows that the nanowires have a surface area of 73.5 m^2/g. The pore size distribution shows a peak at 3.3 nm (Figure 3, also see Supporting Information). The combined properties of porosity and crystallinity for a calcined nanowire are clearly illustrated in the high-resolution TEM (HRTEM) image (Figure 2B).

In order to understand the growth mechanism, we investigated the morphological and structural evolution of the reaction products on Si substrate at different reaction times. We observed that single-crystalline brucite β-$Co(OH)_2$ nanowires first grow on the substrate during the initial 6-h reaction, growing along [001] axis with a diameter of ~200 nm (see Supporting Information). When the reaction time is longer than 6 h, the nanowire surface becomes rough and granular, similar to the morphologies of the final products, and the Co_3O_4 spinel phase starts to appear in the XRD pattern. On the basis of the above observations, we suggest that the granular morphology and the porous texture of the Co_3O_4 nanowires come from the solid-state reaction between the β-$Co(OH)_2$ nanowires and the dissolved oxygen in the solution following the reaction:

$$6\ Co(OH)_2\ (s) + O_2\ (aq) \rightarrow 2\ Co_3O_4\ (s) + 6\ H_2O\ (l)$$

The reorganization of materials during the solid-state reaction results in the formation of mesopores in the product Co_3O_4 phase. The hollow nature of the nanowires might come from the Kirkendall effect,[12] in which an inward flow of vacancies, balancing the outward transport of fast-moving cations, can condense into voids at the center of the nanowire. Such effect has been exploited to synthesize hollow cobalt oxide nanocrystals.[13] Moreover, considering the matched *d*-spacing, we think the above β-$Co(OH)_2$ -to-Co_3O_4 transition is topotactic with the relationship [001] $Co(OH)_2$// [111] Co_3O_4. This can thus explain the growth direction of the final Co_3O_4 nanowires. The topotactical aspect of the oxidation reaction of $Co(OH)_2$ has been reported in previous investigations.[14]

In summary, a facile solution-based synthetic route was developed for the direct growth of porous Co_3O_4 nanowire arrays on various substrates. Their high porosity and surface area can facilitate the contact between external molecules/ions and the oxide surface. The freestanding nanowire arrays with open spaces between individual nanowires allow the easy diffusion of molecules/ions among them. Their direct growth on conductive substrates also facilitates their electric contact with external circuit. These nanowire arrays will, therefore, have promising applications in sensing, Li-ion batteries, and field-emission and electrochromic devices. As a preliminary test, an electrochemical sensor (based on these nanowire arrays) for detecting hydrogen peroxide in aqueous solution has been investigated. The measured current shows a linear dependence on H_2O_2 concentration over a broad concentration region from 5 to 30 mM (see Supporting Information). Other applications in gas sensing and Li-ion batteries are under investigation and will be reported in the future.

Supporting Information Available: Detailed synthetic procedure, FT−IR spectra of the nanowires, morphological and structural evolution of the reaction products, BET measurement, and sensor testing. This material is available free of charge via the Internet at http://pubs.acs.org.

References

(1) Poizot, P.; Laruelle, S.; Grugeon, S.; Dupont, L.; Tarascon, J. M. *Nature* **2000**, *407* (6803), 496−499.
(2) Li, W.-Y.; Xu, L.-N.; Chen, J. *Adv. Func. Mater.* **2005**, *15* (5), 851−857.
(3) Maruyama, T.; Arai, S., *J. Electrochem. Soc.* **1996**, *143* (4), 1383−1386.
(4) Arico, A. S.; Bruce, P.; Scrosati, B.; Tarascon, J.-M.; van Schalkwijk, W. *Nat. Mater.* **2005**, *4* (5), 366−77.
(5) Lakshmi, B. B.; Patrissi, C. J.; Martin, C. R. *Chem. Mater.* **1997**, *9* (11), 2544−2550.
(6) Nam, K. T.; Kim, D.-W.; Yoo, P. J.; Chiang, C.-Y.; Meethong, N.; Hammond, P. T.; Chiang, Y.-M.; Belcher, A. M. *Science* **2006**, *312* (5775), 885−888.
(7) (a) Xu, R.; Zeng, H. C. *J. Phys. Chem. B* **2003**, *107* (46), 12643−12649. (b) Hosono, E.; Fujihara, S.; Honma, I.; Zhou, H. *J. Mater. Chem.* **2005**, *15* (19), 1938−1945.
(8) (a) Feng, J.; Zeng, H. C. *Chem. Mater.* **2003**, 15 (14), 2829−2835. (b) Wang, Y.; Yang, C.-M.; Schmidt, W.; Spliethoff, B.; Bill, E.; Schueth, F. *Adv. Mater.* **2005**, *17* (1), 53−56. (c) Jiao, F.; Shaju, K. M.; Bruce, P. G. *Angew. Chem., Int. Ed.* **2005**, *44* (40), 6550−6553. (d) Hou, Y.; Kondoh, H.; Shimojo, M.; Kogure, T.; Ohta, T. *J. Phys. Chem. B* **2005**, *109* (41), 19094−19098. (e) Yu, T.; Zhu, Y.; Xu, X.; Shen, Z.; Chen, P.; Lim, C.-T.; Thong, J. T.-L.; Sow, C.-H. *Adv. Mater.* **2005**, *17* (13), 1595−1599.
(9) Taberna, P. L.; Mitra, S.; Poizot, P.; Simon, P.; Tarascon, J. M. *Nat. Mater.* **2006**, *5* (7), 567−573.
(10) (a) Li, N.; Patrissi, C. J.; Che, G.; Martin, C. R. *J. Electrochem. Soc.* **2000**, 147 (6), 2044−2049. (b) Patrissi, C. J.; Martin, C. R. *J. Electrochem. Soc.* **1999**, *146* (9), 3176−3180.
(11) Huang, M. H.; Wu, Y.; Feick, H.; Tran, N.; Weber, E.; Yang, P. *Adv. Mater.* **2001**, *13* (2), 113−116.
(12) Smigelskas, A. D.; Kirkendall, E. O. *Trans. AIME* **1947**, *171*, 130−142.
(13) Yin, Y.; Rioux, R. M.; Erdonmez, C. K.; Hughes, S.; Somorjai, G. A.; Alivisatos, A. P. *Science* **2004**, *304* (5671), 711−714.
(14) (a) Figlarz, M.; Guenot, J.; Fievet-Vincent, F. *J. Mater. Sci.* **1976**, *11*, (12), 2267−2270. (b) Pralong, V.; Delahaye-Vidal, A.; Beaudoin, B.; Gerand, B.; Tarascon, J. M. *J. Mater. Chem.* **1999**, *9* (4), 955−960.

JA065308Q